

# INFLUENCE OF DYNAMIC EFFECTS ON POINT EHL CONTACTS IN GEAR SYSTEMS <sup>1</sup>

Marco Barbieri<sup>2</sup>  
Francesco Pellicano<sup>3</sup>

## Abstract

In this paper, the effect of vibrations in elastohydrodynamical lubrication of spur gear pairs will be described. The relevance of inertial effects in the contacting bodies on film fluid lubrication will be clarified with comparisons to static formulations. A new model describing the dynamic behavior of two coupled transient EHL elliptical contacts will be presented and applied to characterize the dynamics of a spur gear pair.

**Keywords:** Gear dynamics; Transient EHL; Multilevel method.

<sup>1</sup> Technical contribution to the First International Brazilian Conference on Tribology – TribobR-2010, November, 24<sup>th</sup>-26<sup>th</sup>, 2010, Rio de Janeiro, RJ, Brazil.

<sup>2</sup> PhD, Università di Modena e Reggio Emilia, Modena, Italy, email: mark@unimore.it

<sup>3</sup> Associate professor, Università di Modena e Reggio Emilia, Modena, Italy, email: francesco.pellicano@unimore.it

## 1 INTRODUCTION

Understanding the dynamic behavior of gear pairs is crucial in order to reduce vibration and noise, and this is especially true for spur gear pairs. For this reason, many approaches have been proposed in the past years to describe the dynamics of gear systems. In 1958, Harris<sup>(1)</sup> proposed a method to reduce vibrations in spur gear pair by means of profile reliefs. Harris assumed that the coupling is stiffer when two pairs of teeth are in contact, more deformable when only one couple is mating. In 1990, Kahraman and Singh<sup>(2)</sup> described the dynamics of a spur gear pair using a 1 dof lumped parameter model like that depicted in

Figure 1 (a). The 1 dof model was validated by Kahraman and Blankenship,<sup>(3)</sup> who also proved the effectiveness of profile modifications in reducing gear vibrations. In the last years, many models for gear dynamics were proposed, taking into account misalignments, profile errors or the full transmission, but relatively a few efforts were done to characterize the damping coefficient  $c_g(t)$ . Figure 1 (b), shows the amplitude-frequency diagrams for a case study (see Barbieri<sup>(4)</sup> for more details): varying the damping coefficient, the response of the system can be either fully linear or can present a non-linear softening behavior due to loss of contact in the mating teeth pair.

To study the damping effect in the spur gear pair, it is necessary to consider the lubricant between the surfaces in contact. The lubrication regime for industrial gear systems is elastohydrodynamic, i.e. it is necessary to keep into account local deformation in the contacting surfaces due to lubricant pressure to obtain a proper estimation of oil pressure and minimum film thickness. Indeed, since the first results due to Grubin<sup>(5)</sup> in 1949, coupling between Reynolds equation and the elastic deformation integral was applied to gears, since the minimum film thickness obtained from EHL computation was high enough to explain the reduced wear rate measured on tooth flanks. In more recent times, the problem of transient EHL lubrication in gear pairs, i.e. taking into account the squeeze term of the Reynolds equation, has been faced by many authors. In 1997, Larsson<sup>(6)</sup> presented a solution for the lubricated line contact problem under a square-wave load, to simulate the varying number of teeth in contact. In 2004, Wang, Li and Yang<sup>(7)</sup> used a trapezoidal varying load and took into account thermal effects and non-Newtonian lubricants.

All the literature found on this problem solve a static equilibrium equation, together with Reynolds equation and the elastic integral deformation, in order to find the rigid-body approach, so they completely neglect inertial effects. The purpose of this paper is to show what happens to the film thickness and to the rigid body approach, if inertial effect are taken into account. It is to note that the rigid body approach is the Dynamic Transmission Error DTE of the gear pair, and is a direct indicator of the vibration level.

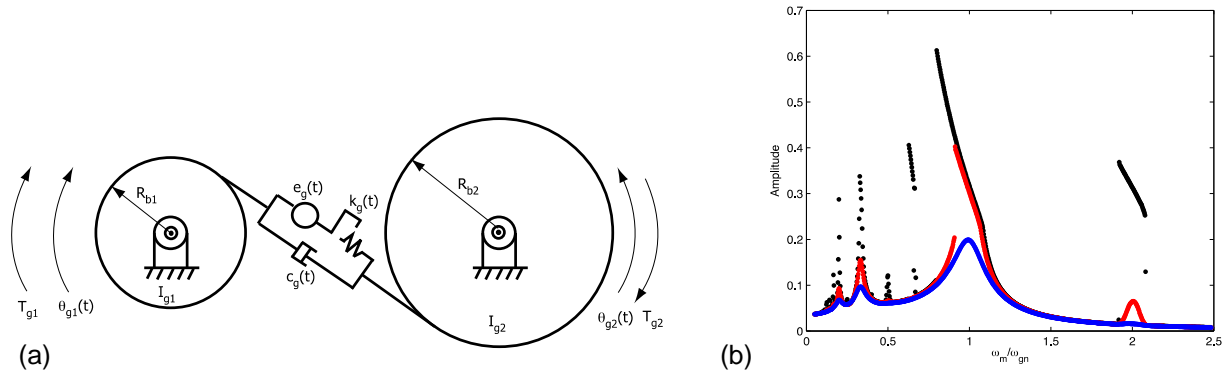


**Figure 1:** (a) Lumped parameter model for spur gear dynamics; (b) Amplitude-frequency diagram for different values of the non-dimensional damping coefficient (0.01 black, 0.05 red, 0.1 blue)

## 2 METHODS

The problem of transient EHL will be solved for the point contact, so that the effect of gear crowning can be considered. Transient Reynolds equation reads:

$$\frac{\partial}{\partial x} \left( \frac{\rho h^3}{12\eta} \frac{\partial p}{\partial x} \right) + \frac{\partial}{\partial y} \left( \frac{\rho h^3}{12\eta} \frac{\partial p}{\partial y} \right) - u_m \frac{\partial}{\partial x} (\rho h) - \frac{\partial}{\partial t} (\rho h) = 0 \quad (1)$$

where  $u_m$  is the mean velocity of the mating profiles and varies linearly during tooth contact.

Film thickness is computed as follows:

$$h = h_0 + \frac{x^2}{2R_x} + \frac{y^2}{2R_y} + \frac{2}{\pi E'} \iint_{-\infty}^{\infty} \frac{p(x', y', t) dx' dy'}{\sqrt{(x-x')^2 + (y-y')^2}} \quad (2)$$

where  $R_x$  is the equivalent radius of curvature in the profile direction and  $R_y$  along the face width.  $R_y$  is constant during tooth meshing, while  $R_x$  is varying with quadratic law. Figure 2 explains the meaning of these parameters; note that equivalent radii are referred to a contact between a parabolic surface and a plane: the relationship among the true radii of curvature and the equivalent ones is the same as in standard Hertz's theory. Roelands pressure-viscosity relationship and Dowson and Higginson density-pressure formula are used to compute the dynamic viscosity  $\eta$  and density  $\rho$ .  $\alpha_B$  will be assumed equal to  $2.2 \cdot 10^{-8}$ .

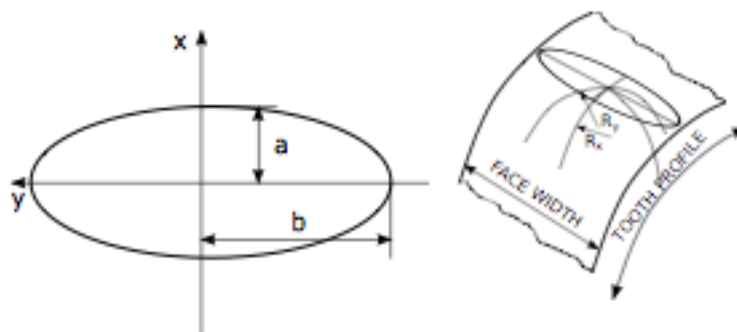


**Figure 2:** Contact ellipse and sketch of the equivalent tooth profile.

All dimensionless quantities will be defined with respect to the hertian point contact solution, as done in Nijenbanning, Venner e Moes<sup>(8)</sup> for the stationary case. Here, since many parameters change during meshing, a reference position for the gear system is to be chosen: the pitch point is the natural choice. P is made dimensionless dividing by the maximum hertian pressure  $p_h$  at the pitch point, X and Y are divided by the minor half axis  $a^*$  of the hertian contact ellipse, so the non-dimensionalization is as in the following:

$$\begin{aligned} X = \frac{x}{a^*} \quad ; \quad Y = \frac{y}{a^*} \quad ; \quad H = \frac{R_x}{a^2} h \quad ; \quad P = \frac{\rho}{\rho_h^*} \\ \bar{\eta} = \frac{\eta}{\eta_0} \quad ; \quad \bar{\rho} = \frac{\rho}{\rho_0} \quad ; \quad U_m = \frac{t^*}{a^*} u_m \quad ; \quad T = \frac{t}{t^*} \end{aligned} \tag{3}$$

where  $t^*$  is to be defined so that the number of parameters is reduced to a minimum. The best choice is to obtain equal coefficients for the *Couette* and the *Squeeze* term inside the Reynolds equation:  $t^* = a^* / u_m$ . The resulting dimensionless equations are:

$$\begin{aligned} \frac{\partial}{\partial X} \left( \bar{\xi} \frac{\partial P}{\partial X} \right) + \frac{\partial}{\partial Y} \left( \bar{\xi} \frac{\partial P}{\partial Y} \right) - \frac{\partial}{\partial X} (\bar{\rho} H) - \frac{\partial}{\partial T} (\bar{\rho} H) = 0 \\ \bar{\xi} = \frac{\bar{\rho} H^3}{\lambda \bar{\eta}} \quad \text{where} \quad \lambda = \frac{12 u_m \eta_0 R_x^2}{a^{*3} \rho_h^*} \end{aligned} \tag{4}$$

$$H = H_0 + \frac{1}{R_x} \frac{X^2}{2} + D^* \frac{Y^2}{2} + \frac{2}{\pi^2} \chi_{\rho_h^*} \int_{-\infty}^{\infty} \int_{-\infty}^{\infty} \frac{\rho(X', Y', T) dX' dY'}{\sqrt{(X - X')^2 + (Y - Y')^2}}$$

where  $\chi_{\rho_h^*}$  is a correction for the elliptical case and requires the numerical or approximated computation of elliptical integrals (see Barbieri<sup>(4)</sup>).  $\bar{R}_x$  is the ratio between the radius of curvature along the profile in a given position and the value at the pitch point;  $D^*$  is the ratio between  $\bar{R}_x$  and  $\bar{R}_y$  at the pitch point. This set of equations is to be completed by an equilibrium equation, if the external load is given and the rigid-body approach  $h_0$  is to be determined. If the external load is not given, the equation of motion is to be solved. In the case of gear application, when contact ratio is in the range 1-2, one or two EHL lubricated contact can exist at the same time. Figure 3 (a) shows the most general case: static load  $T_{g1}/R_{b1}=T_{g2}/R_{b2}$  and dynamic load due to the rotary inertias of the wheels  $I_{g1}$  and  $I_{g2}$  are shared by EHL contact 1 and 2.

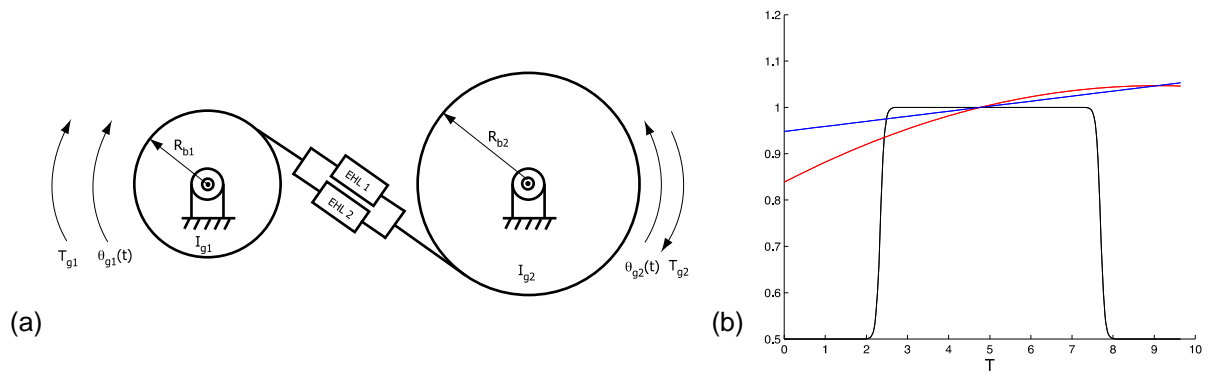


**Figure 3:** (a) Full model for EHL gear problem; (b) Parameters during contact:  $f(T)$  black,  $\bar{R}_x$  red,  $\bar{U}_m$  blue.

The equation of motion on the line of action, for the system in Figure 3 (a) is:

$$m_{ge} \frac{d^2 h_0}{dt^2} = \int_{-\infty}^{\infty} \int_{-\infty}^{\infty} P_1(x, y, t) dx dy + \int_{-\infty}^{\infty} \int_{-\infty}^{\infty} P_2(x, y, t) dx dy + \frac{T_{g1}}{R_{b1}} \quad (5)$$

where  $P_1$  and  $P_2$  are the pressure distributions related to the two lubricated contacts,  $T_{g1}$  is constant and  $m_{ge}$  is the equivalent mass (see Kaharaman<sup>(2)</sup> for details), given by the following formula:

$$m_{ge} = \left( \frac{R_{b1}^2}{I_{g1}} + \frac{R_{g2}^2}{I_{g2}} \right)^{-1} \quad (6)$$

With the proposed formulation, the EHL problem is to be solved alternately for one or two contacts during meshing: assuming that the load is equally shared by both contacts, it is possible to study a simplified problem for only one contact. Eq. (7) is the motion equation for only one contact:  $f(t)$  is a time varying parameter as in Figure 3 (b). The same figure shows value for the other parameters  $\bar{R}_x$  and  $\bar{U}_m$  starting from entering contact ( $T=0$ ) up to contact exit.

$$m_{ge} \frac{d^2 h_0}{dt^2} = \frac{1}{f(t)} \int_{-\infty}^{\infty} \int_{-\infty}^{\infty} P(x, y, t) dx dy + \frac{T_{g1}}{R_{b1}} \quad (7)$$

Eq. (7) can be made non-dimensional by introducing a dimensionless inertia parameter  $l$ :

$$l = \frac{m_{ge}}{R_x^* t^{*2} p_h^*} = \frac{2\pi m_e u_m^{*2}}{3R_x^* w^* \kappa^*} \quad (8)$$

$$l \frac{d^2 H_0}{dT^2} = \frac{1}{f(T)} \int_{-\infty}^{\infty} \int_{-\infty}^{\infty} P(X', Y', T) dX' dY' - \frac{2\pi}{3\kappa^*}$$

where  $\kappa^* = a^*/b^*$  is the ellipticity ratio at the pitch point and  $w^*$  is the static load at the pitch point. It is to note that the aforementioned literature cases, which consider only one contact and the equilibrium equation, can be reproduced by letting  $l=0$ . The only difference is the kind of contact, which is a point contact in the present

approach, a line contact in literature. Numerical solution of the problem is obtained by means of the multilevel technique proposed by Lubrecht<sup>(9)</sup> for the stationary problem, which consists in a multigrid iterative solver for the Reynolds equation, coupled with a multilevel fast-integration algorithm for computing the discretized integral in (2). The equation of motion is solved iteratively, using an implicit Adam-Bashfort algorithm. In order to minimize the number of parameters and to obtain results that are easy to compare with literature, it is useful to introduce Moes' parameters, which are defined in Moes and Bosma<sup>(10)</sup> for the circular stationary case.

$$M = \frac{w^*}{E'R_x^2} \left( \frac{2\eta_0 u_m^*}{E'R_x^*} \right)^{-\frac{3}{4}} = \frac{T_{g1}}{R_{b1}^3 \tan^2(\alpha')} \left( \frac{(1+\tau)^5}{8\eta_0^3 E\Omega_1^3} \right)^{\frac{1}{4}} \tag{9}$$

$$L = \alpha_B E' \left( \frac{2\eta_0 u_m^*}{E'R_x^*} \right)^{\frac{1}{4}} = \sqrt[4]{2\eta_0 \alpha_B^4 E'^3 \Omega_1 (1+\tau)}$$

Using Moes' parameters, the non stationary problem is fully defined by non dimensional inertia I and the time varying parameters  $\bar{R}_x$ ,  $\bar{U}_m$  and  $f(t)$ .

### 3 RESULTS

A comparison among the static approach, i.e. I=0, and the two proposed dynamic models, single or double contact, is presented in this section for the case study summarized in Table 1.

**Table 1:** Data for the case study

Data	Symbol	Pinion	Gear
Number of teeth	$Z$	28	43
Module [mm]	$m$	3	3
Pressure angle [Deg]	$\alpha$	20	20
Base radius [mm]	$R_b$	39.467	60.610
Theoretical pitch radius [mm]	$R_p$	42	64.5
Thickness on theoretical pitch circle [mm]	$s_p$	6.1151	6.7128
Addendum modification [mm]	$v$	1.927	2.748
Outer diameter [mm]	$R_a$	93.1	139.7
Root diameter [mm]	$R_f$	79.1	126.2
Crowning magnitude [mm]	$mag_c$	0.020	0.020
Face width	$F_w$ [mm]	20	20
Inertia [kg m <sup>2</sup> ]	$I_g$	0.0008076	0.0047762
Young's modulus [MPa]	$E$	206000	206000
Poisson's coefficient	$\nu$	0.3	0.3
Center distance [mm]	$a'_g$	111	
Backlash [mm]	$j_n$	0.3461	
Backlash on the line of action [mm]	$j_n$	0.312	
Transmission ratio	$\tau$	0.6511	
Contact ratio	$\varepsilon_\alpha$	1.28565	
Torque [Nmm]	$T_{g1}$	470000	

Moes' parameters defined in Moes and Bosna<sup>(9)</sup> allow to clarify the lubrication regime at which the gear pair operates (Figure 4): in the operating range, between 1000 and 20000 pinion RPM, M is comprised between 1600 and 18000 and L is

between 14 and 30. These parameters correspond to the elastic-piezoviscous lubrication regime, that means the contact is highly loaded and highly hydrodynamic, thus both elasticity and piezo-viscosity cannot be neglected (here Roelands formulation is adopted).

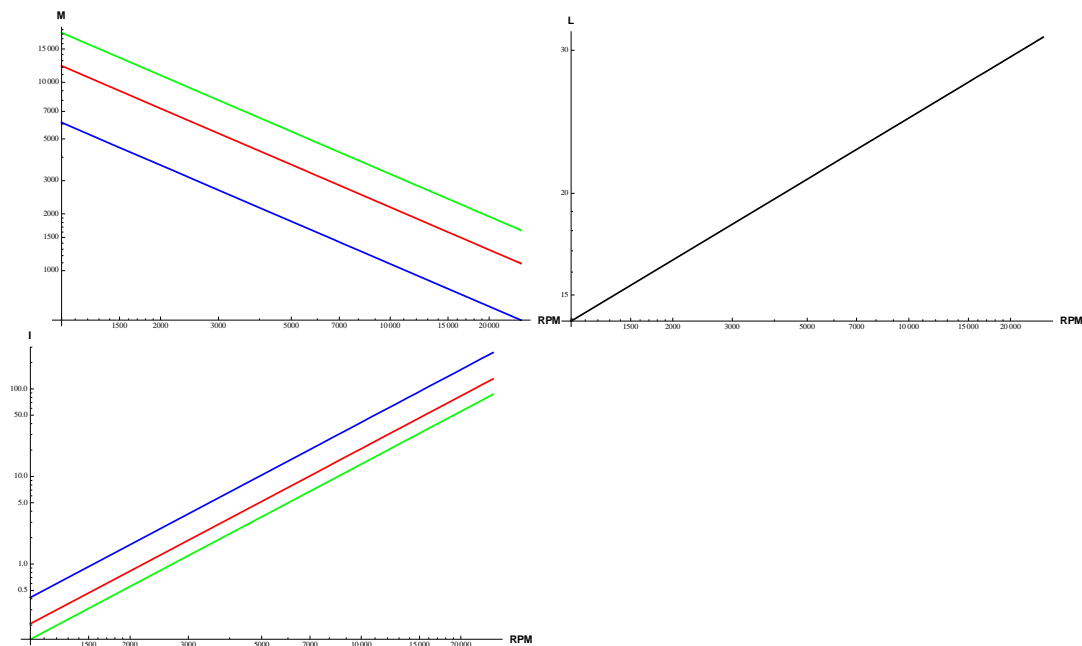


**Figure 4:** Parameter dependence over pinion RPM and load level: green - nominal load  $T_{g1}$ ; red – 66%  $T_{g1}$ ; blue – 33%  $T_{g1}$ .

Figure 5 presents the results obtained from time integration of equation (8) when inertia is artificially set to zero, so that the results can be compared with literature. The contact is studied from the entering to the exit; of course it is necessary to define initial conditions for pressure and rigid approach  $h_0$ : here stationary film fluid is assumed, thus neglecting the effect of film build-up. Small oscillations in central pressure and film thickness can be observed close to the abrupt load variation defined in Figure 3 (b); there is not much dependence on the rotating speed of the pinion, except for the film thickness: higher rotational speeds produce higher lift force and the film thickness increases.

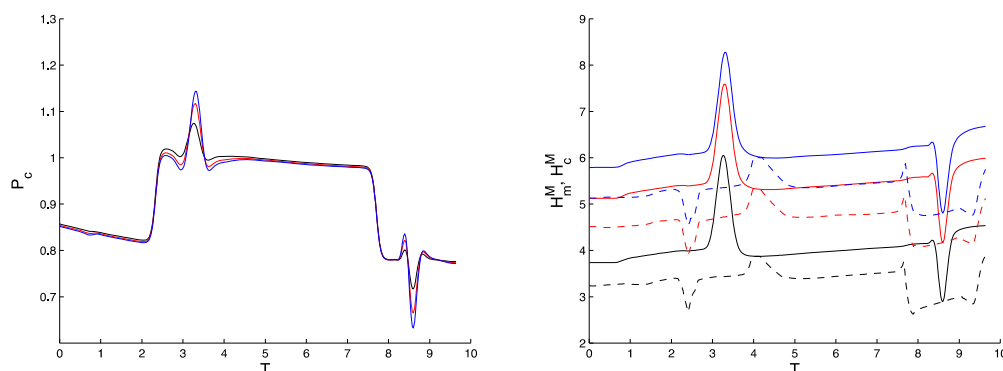


**Figure 5:** Central pressure  $P_c$  and minimum  $H_m$  (- -) and central  $H_c$  (—) film thickness in the static case: black - 2500 RPM, red – 7500 RPM, blue – 12500 RPM.

Figure 6 shows the effect of introducing the equivalent inertia in the (8); as before, stationary film fluid is assumed as initial condition. It can be seen that the change in

$f(t)$ , now introduce an oscillation in the fluid pressure and in the film thickness, and that the period of this oscillation increases with pinion speed increase. Of course it is the relative period to be incremented, because the dynamic of the system is faster, so that for pinion rotational speed over 7500 RPM no oscillation can be observed, but the fluid cavitates over all the contact. Even though  $h_0$  obtained from time integration could be assumed as Dynamic Transmission Error, the main limitation of this approach is that the simulation cannot be studied after the exit contact, so it is necessary to switch back to the two contact problem stated in eq. (5).

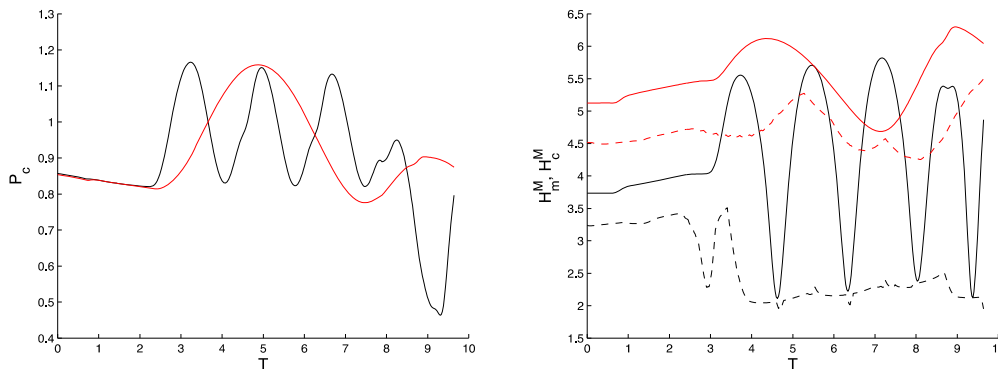


**Figure 6:** Central pressure  $P_c$  and minimum  $H_m$  (- -) and central  $H_c$  (-) film thickness in the dynamic, one contact case: black - 2500 RPM, red – 7500 RPM.

For the two contact problem, initial conditions are set up at the pitch point, where only one pair of teeth is in contact: stationary condition is imposed for contact  $EHL_1$  then contact  $EHL_2$  enters at the proper time, inheriting the actual rigid body approach  $h_0$  computed for  $EHL_1$ . Later on,  $EHL_1$  exits and is then replaced by another occurrence of  $EHL_1$  so that time simulation can be continued.

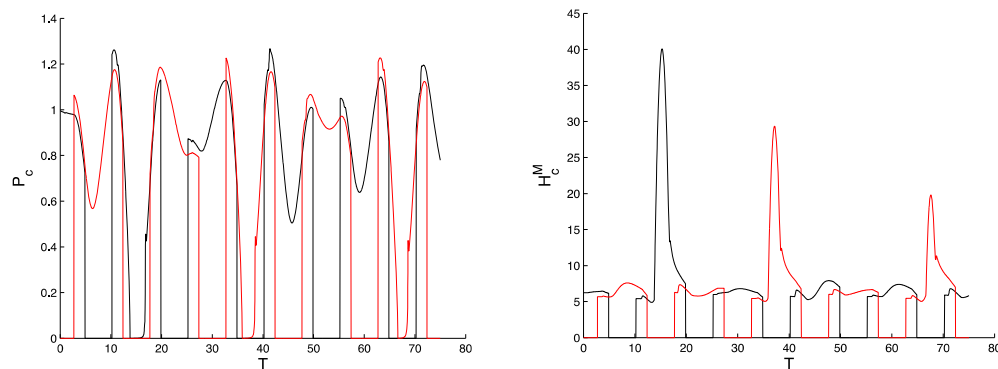


**Figure 7:** Central pressure  $P_c$  and central  $H_c$  film thickness in the dynamic, two contact case: 15000 RPM.

Figure 7 displays the results of time integration: black line is contact  $EHL_1$ , red line is contact  $EHL_2$ . The proposed approach allows to continue the integration after the exit of one contact, cavitation on the full contact occurs due the initial condition chosen. This analysis can also give reason of the hypothesis of equal load subdivision between the contacts: Figure 8 (a) shows the integrals of the two pressure distributions during time. Whenever two contacts are active, the load on each one is almost the same, so that the simplified one contact approach is only affected by the issue of finding proper initial conditions, since it is impossible to follow



the contact for a long time. Figure 8 (a) displays the rigid-body approach, which, in the proposed model, is a direct measure of the Dynamic Transmission Error.

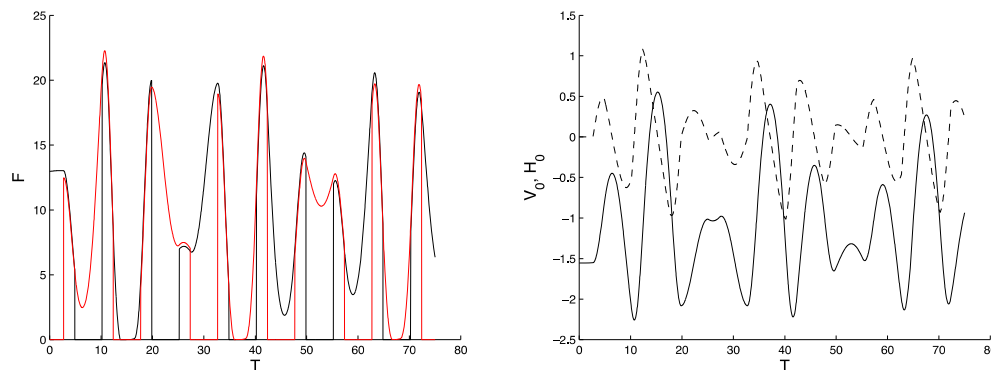


**Figure 8:** Integral of pressure; rigid-body approach  $h_0$  and its derivative  $v_0$ , two contact case: 15000 RPM.

#### 4 DISCUSSION AND CONCLUSION

Different approaches to study the problem of EHL lubrication in spur gear pairs have been compared focusing on the dynamic effect. Results from dry dynamic models used in literature were taken into account as reference: since in industrial application, vibrations and eventually loss of contact occur, EHL models for gear pair cannot neglect the inertias of contacting bodies. The analysis shown without inertia presents only small oscillations both for pressure and film thickness and these oscillations are due to squeeze effect in the film fluid. The effect of gear vibrations is much more important, as can be seen solving Newton's equation instead of the equilibrium equation. Nevertheless, this approach is not complete either, because it allows to study only one contact, from the enter to the exit, and the result is strongly dependent on the initial condition, which are unknown. To obtain proper results, both for studying the lubrication condition in gear pairs and to compute the damping effect due to the fluid, it is necessary to consider the coupling of two EHL contacts, sharing the same rigid-body approach.

#### Acknowledgements

This work was developed during a visiting term ad the INSA Lyon, with the great help of Prof. A.A. Lubrecht for developing the Multilevel solver.

#### REFERENCES

- 1 HARRIS, S.L., **Dynamic Loads on the Teeth of Spur Gears**, Proceedings of the Institution of Mechanical Engineers, 172(2), pp. 87-100, 1958.
- 2 KAHRAMAN, A., SINGH, R., **Non-linear Dynamics of a Spur Gear Pair**, Journal of Sound and Vibrations, 142 (1), pp. 49-75, 1990.
- 3 KAHRAMAN A., BLANKENSHIP G. W., **Effect of Involute Tip Relief on Dynamic Response of Spur Gear Pairs**, Journal of Mechanical Design, 121, pp. 313-315, 1999.
- 4 BARBIERI, M., **Gear Dynamics Under EHL Conditions**, PhD Thesis, Università di Modena e Reggio Emilia, Modena, Italy, 2010.
- 5 GRUBIN A.N., **Fundamentals of the Hydrodynamic Theory of Lubrication of Heavily Loaded Cylindrical Surfaces**, Moscow: TsNIITMASH, Book 30 (Engl. transl.), 1949.
- 6 LARSSON, R., **Transient non-Newtonian Elastohydrodynamic Lubrication Analysis of an Involute Spur Gear**, Wear, 207, 67-73, 1997.

- 7 WANG, T., LI H., TONG, J., YANG, P., **Transient Thermoelastohydrodynamic Lubrication Analysis of an Involute Spur Gear**, Tribology International, 37, 2004.
- 8 NIJENBANNING G., VENNEN C.H., MOES H., **Film Thinckness in Elastohydrodynamically Lubricated Elliptic Contacts**, WEAR, 176, pp.217-229, 1994.
- 9 LUBRECHT A.A., **Numerical Solution of the EHL Line and Point Contact Problem Using Multigrid Techniques**, Ph.D. Thesis, University of Twente, Enschede, The Netherlands ISBN 90-9001583-3, 1987.
- 10 MOES H., BOSMA R., **Design Charts for Optimum Bearing Configuration, I the Full Journal Bearing**, ASME J. of Tribology, 93, pp.302-306, 1971.